Composites with Recovered Polystyrene Reinforced with Pine or Poplar Residues Following Lignin Extraction

Orhan Kelleci

Email: orhankelleci@ibu.edu.tr

DOI: 10.15376/biores.20.4. 9184-9207

GRAPHICAL ABSTRACT

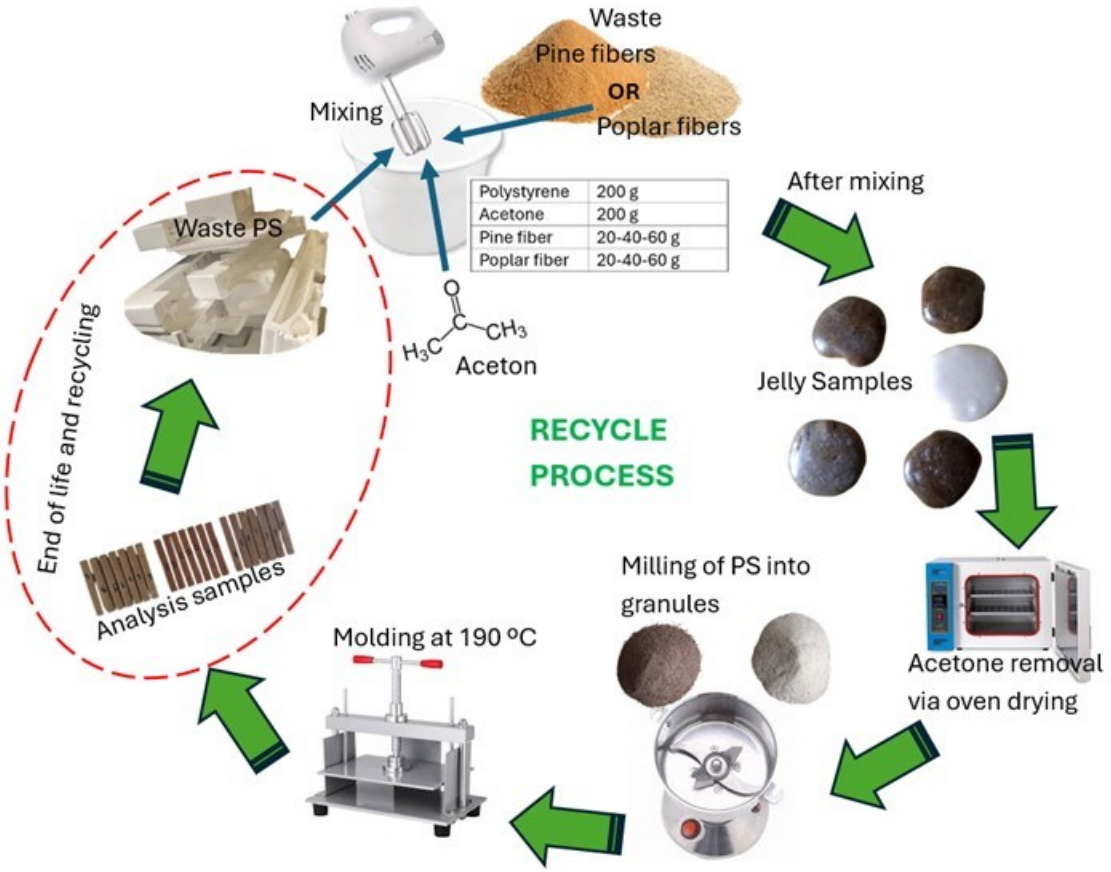

Composites with Recovered Polystyrene Reinforced with Pine or Poplar Residues Following Lignin Extraction

Orhan Kelleci

Sustainable composites were produced by recycling polystyrene (PS) and pine and poplar fiber residues remaining after lignin extraction. Polystyrene was dissolved in acetone and reinforced with wood fiber residues at 10%, 20% and 30%. The mixture was dried at 100 °C for 2 hr, granulated, and pressed at 190 °C under 5 MPa for 20 minutes. Characterizations of samples were performed according to physical (ASTM D1037 for water resistance and ASTM 7032-21 for density measurement), mechanical (ASTM D638 for tensile, ASTM D790 for flexural), scanning electron microscopy (SEM), X-ray diffraction (XRD), and Fourier transform infrared spectroscopy (FTIR) analyses. The addition of fiber residue increased (up to 6.7%) the density but decreased the water absorption (WA) (up to 22%) and thickness swelling (TSW) (up to 12%). Fiber residue increased tensile strength (TS) by 46 to 167% and flexural strength (FS) by 45 to 82%. However, it decreased tensile modulus (TM) by 0 to 58% and flexural modulus (FM) by 3 to 12% (excluding pine). However, pine fiber residue increased FM by 2 to 19%. SEM analyses revealed homogeneous distribution of fiber residues.

DOI: 10.15376/biores.20.4.9184-9207

Keywords: Polystyrene; Recycled composites; Lignin extraction; Poplar fiber; Pine fiber

Contact information: Forestry Department, Mudurnu Sureyya Astarci Vocational School, Bolu Abant Izzet Baysal University, P. O. Box 14100, Bolu, Türkiye; Email: orhankelleci@ibu.edu.tr

INTRODUCTION

The excessive increase in the human population in the last 300 years has caused a change in understanding the idea of consumption. Especially after the industrial revolution, the world's natural resources have started to be consumed rapidly (Pollard 1958; Calvin *et al.* 2023). Previously, a linear production model (take–make–dispose) was prevalent; however, current approaches are shifting toward circular and sustainable production models. For this reason, it has become important to produce upcycled products. Conscious people have begun to wonder about the source of the products they consume, and the demand for recycled products has increased (Tansel 2020). Today, products produced from recycling have been attracting more attention. It is predicted that there will be more demand for recycled products in the future because environmental pollution in the world has reached dangerous levels.

The definition of environmental pollution was first brought to the agenda in 1869 by the Public Health Committee of the State of Massachusetts, USA, and in the published declaration, it was emphasized that every individual needed vital resources such as clean air, water and soil, and that these resources should not be polluted (Massachusetts General Court 1869; Kramer 1950; Gündüz 2013). Materials that disrupt the natural balance of the

environment and negatively affect the biological activities of living things can be considered as pollutants. Today, one of the most important pollutants that causes environmental pollution is plastic (Verhaar *et al.* 1992).

Over the last 70 years, plastic production has increased dramatically, with a total of 8.3 billion tons of plastic produced (Rhodes 2019). The majority of this production is directly released into the environment: only 9% of plastic waste is recycled, 12% is incinerated, and the remaining 79% is landfilled or released into nature (Milbrandt *et al.* 2022). Packaging waste, in particular, accounts for one third of plastic consumption, and much of it is distributed uncontrolled into the environment. Microplastics have been detected in 92% of drinking water samples in the USA and 72% in Europe (De Frond *et al.* 2022). These particles have even been found in human lung tissue and remote mountain soils. This situation necessitates an urgent restructuring of plastic production and waste management on a global scale.

To prevent plastic pollution, legislators are taking various measures. For example, the European Chemicals Agency (ECHA) recently adopted restrictions on intentionally added microplastics (ECHA 2023), and the European Union has proposed the Packaging and Packaging Waste Directive (PPWR 2023), which aims to make all packaging recyclable or reusable by 2030 (European Commission 2023).

One of the most important plastic pollutants is expanded polystyrene (EPS) or extruded polystyrene (XPS). This plastic material is widely used in single-use items for the packaging industry. Such items are used once and then thrown away. If these wastes are not disposed of with appropriate methods, they cause environmental pollution and negatively affect human, animal and plant health. It has been emphasized that styrene oligomers (SOs) are found in high concentrations in various regions, especially in industrial areas and urban coasts, and that SOs in particular can cause ecotoxic effects even at low concentrations (De-la-Torre *et al.* 2020). In another study, Kwon *et al.* (2015) collected seawater and sand samples from 244 coastal locations in 21 countries between 2003 and 2013 and measured the amounts of styrene monomer (SM), dimer (SD) and trimer (ST) compounds derived from PS in these samples. Experimentally, when they tested how these pollutants leach from the PS surface under laboratory conditions, they found much higher amounts of SOs in the sand samples than in seawater. Polystyrene also causes serious pollution in the soil of wetlands.

Kukharchyk and Chernyk (2022) conducted a study in the affected area of a factory producing EPS insulation boards in Minsk, Belarus, and detected polystyrene particles in both the soils surrounding the industrial site and the alluvial soils of the river floodplain downstream of the factory. Microplastics were found in the industrial site soil in the range of 31 to 175 particles/kg, while in the alluvial soil of the river floodplain, this value reached 94 to 8864 particles/kg. The researchers explain the higher accumulation of microplastics in alluvial soils by the fact that water flow and flood processes entrain and deposit particles in these areas. This suggests that soil type and hydrological processes play an important role in the distribution of microplastic pollution. Also, polystyrene microplastic pollutants have been found to have significant toxic effects on both marine organisms and human blood cells. In particular, it has been found that they cause morphological deterioration and oxidative stress in *Artemia salina* and DNA damage in human lymphocytes (Mishra *et al.* 2019; De-la-Torre *et al.* 2020).

The increase in environmental concerns and the increase in human needs at the same time emphasize how important recycling is. The composite industry has a raw material supply problem, and the number of products produced from recycled EPS and

XPS is increasing day by day. When considered from this perspective, many studies are being conducted on the production of new composite materials from recycled polystyrene and the determination of their characterization.

Table 1. Previous Studies That Used Different Fillers or Reinforcements with Polystyrene in Literature

Study	Filler type	Matrix	Filler ratio (%)	Method	Results
Singha & Rana (2012)	*Agave americana* fibers (raw and modified with MMA)	PS	10–30	Compression molding	20% filler is optimal; With surface modification, TS and FS has increased, thermal stability has improved.
Flores-Hernández *et al.* (2017)	*Eucalyptus globulus* talaşı	PS	10–50	Extrusion + Thermo-Compression	The small particle size provided a higher Young's modulus; Water absorption increased, melt flow index decreased.
Kaho *et al.* (2020)	Mixed carpentry shop wood waste	EPS	15–30	Aseton Dissolving + thermoforming	As the resin ratio increased, water absorption and porosity decreased; Thermoformed samples showed a more homogeneous structure.
Eroğlu *et al.* (2023)	*Sorghum halepense* (leaf and stem) fibers	Recycled PP	10–30	Extrusion + molding	The fiber additive increased the modulus of elasticity but decreased the TS; SEM analysis showed good fiber distribution.
García-Sobrino *et al*. (2023)	Recycled-EPS	EPS	-	Acetone solubilization + 3D printing (DIW)	EPS maintained its structural integrity in physical recycling; In 3D printing, a homogeneous and reproducible structure was obtained.
Ugwu & Obele (2023)	EPS waste	EPS	-	Mechanical, chemical, thermal recycling	EPS recycling methods and different applications (building materials, asphalt, paint) were summarized.
Köksal & Kelleci (2024)	MDF powder and fiberglass	PS	50–150	Gasoline dissolving + press molding	Glass fiber screw increased TS; MDF filler increased water absorption values.

Manikandan Nair *et al.* (1996) found that in polystyrene composites reinforced with benzoylated sisal fibers, significant improvements were achieved in TS and TM with increased matrix compatibility. They emphasized that the products produced with this method would be advantageous in terms of cost advantage, biodegradability, and low density. Singha and Rana (2012) stated that methyl methacrylate (MMA) modified agave fiber reinforced polystyrene composites exhibited optimum mechanical properties at 20% fiber loading, making them suitable for engineering applications such as construction, automotive, and packaging. In their study, Garcia-Sobrino *et al.* (2023) physically recycled EPS by dissolving it in acetone with Direct Ink Write (DIW) 3D printing technology and demonstrated that this method has the potential for reuse in areas such as packaging, prototyping, and architectural design due to its low cost and accessibility. Kaho *et al.* (2020) developed a composite material using recycled EPS and mixed wood chips obtained from carpentry shops. They did not distinguish a specific wood species in their study; they focused more on general carpentry waste. Additionally, prepared solutions were used as a

binder, and composites were prepared with EPS at different volume fractions (15%, 20%, 25%, and 30%). The present study, on the other hand, presents a species-based approach, evaluating pine (*Pinus nigra* Arnold) and poplar (*Populus alba* L.) wood fiber residues separately and using fiber residues obtained from lignin extraction as raw materials. In this respect, the present work differs from that of Kaho *et al.* (2020) in terms of both the identification of the wood species used and the evaluation of lignin industry by-products. Literature reports that cellulosic reinforcements in polystyrene composites without compatibilizers generally reduce strength properties (*e.g.*, modulus of rupture). However, this study hypothesized that adding pine and poplar fiber residues without compatibilizers but with the solubilization of the polystyrene in acetone could improve the mechanical strength through stress transfer resulting from matrix interactions In many similar studies (Table 1), polystyrene composites were reinforced with different fillers and intended to be used for different purposes.

In the presented study, unlike other studies, all materials including fillers were recycled materials or by-products from another industry. Polystyrene was picked up from a garbage container. Pine and poplar fiber residues remaining from lignin extraction were used as fillers. Recycled EPS and XPS were dissolved using acetone and pine and polar fiber residues were added to the solution at certain rates and wood plastic composites was prepared. No extruder was used in the preparation of the samples. Samples were prepared in a hot press. Maleic Anhydride Grafted Polypropylene (MAPP) (a widely used compatibilizing agent) was not used in the preparation of the samples.

EXPERIMENTAL

Materials

The recycled EPS and XPS used in the study were picked up from waste bins in Bolu/Türkiye. XPS and EPS densities were 10 to 20 kg/m^3 packaging waste. Acetone used for dissolving PS was purchased from Edulap company in Ankara/Türkiye. Some technical properties of PS are given in Table 2.

Table 2. Some Technical Properties of PS

Property	Value (Typical)
Appearance	Solid (amorphous)
Color	White or transparent
Odor	Odorless
Density (20 °C)	~1.04 to 1.06 g/cm³
Glass Transition Temperature (Tg)	~95 to 105 °C
Melting/Softening Point	Amorphous – softens at ~240 °C
Solubility in Water	Insoluble
Solubility in Organic Solvents	Soluble in benzene, toluene, acetone
Auto-Ignition Temperature	~490 °C
Decomposition Temperature	>350 °C (thermal degradation)

The fiber residues remaining from lignin extraction were obtained from Bartın University laboratory. Lignin from *Pinus nigra* Arnold and *Populus alba* L. wood was obtained by an environmentally friendly method using choline chloride and lactic acid

based deep eutectic solvent; the remaining part was used as filler in polystyrene. As reported in the literature, as a result of the delignification process, ~20 to 25% lignin, ~45 to 50% cellulose, and ~20 to 25% hemicellulose remained in poplar fiber residues, while pine fiber residues typically contain ~27 to 30% lignin, ~40 to 45% cellulose, and ~25 to 30% hemicellulose (Wang *et al.* 2020). Lignin production was not related to this study. What was related to this study was the use and characterization of the remaining lignin in PS composites.

Preparation of Samples

No additional post-treatment was applied to remove the chemicals used during lignin extraction. This is primarily due to the negligible chemical residues remaining on the fiber residue surface. Furthermore, these residues are expected to be largely inert and will evaporate or decompose during the high temperature pressing (190 °C) conditions applied during composite production. Therefore, no additional washing or neutralization steps were deemed necessary. Waste PS was cleaned from dirt and dust. It was cut into (100 mm x 100 mm) small pieces. PS pieces were put into a plastic container with acetone solvent (Fig. 1a). Then 200 g of acetone was used to dissolve 200 g of PS. After PS was dissolved, it turned into a gel-like state (Fig. 1b). Pine and poplar fiber residues were added to the gel-like PS/acetone solution at 10, 20, and 30% levels. Fiber residues and solution were mixed (200 rpm) for 10 min using a mechanical mixer. Then, sample mixtures were prepared. The production recipes (sample pattern) of the samples are given in Table 3.

Table 3. Experimental Design

Samples	Waste PS (g)	Acetone (g)	Pine fiber residue (g)	Poplar fiber residue (g)
Neat PS	200	200	0	0
10%Pine	200	200	20	0
20%Pine	200	200	40	0
30%Pine	200	200	60	0
10%Poplar	200	200	0	20
20%Poplar	200	200	0	40
30%Poplar	200	200	0	60

Acetone was removed from the prepared mixtures. The mixtures were poured onto a Teflon plate as a thin layer and left for 2 hr at room temperature (Fig. 1c). Acetone was still trapped in the inner parts of the matrix. Hardened mixture samples were cut into 10 mm x 10 mm x 3 mm pieces using scissors (Fig. 1d). To fully remove the acetone from the samples, the samples were kept in the oven at 100 ºC for 2 hr (Fig. 1e). Then, the mixture was ground in a 20000 rpm mill and kept in the oven again (Fig. 1f). This baking and grinding process was continued until the samples did not increase in volume (approximately 3 times). In this way, acetone in the samples was largely removed (according to the results of weight measurements).

Finally, the samples were ground in the mill and turned into 0.2 to 0.8 mm thick granules. These granules were poured into 140 mm x 90 mm x 3.2 mm mold and pressed in a hot press at 5 MPa for 5 min (Fig. 1g). After hot pressing, the samples were kept at room temperature for 1 h to ensure dimensional stability (Fig. 1h). Sample sheets with dimensions of 140 mm x 90 mm x 3.2 mm were cut to dimensions of 130 mm x 13 mm x

3.2 mm using a diagonal saw so that analysis samples were prepared (Fig. 1i). Then, samples were characterized by physical, mechanical (Fig. 1k) and morphological.

Fig. 1. Sample preparation process, waste PS and acetone solvent (a); PS in a gel-like state (b); gel-like blend (c); at room temperature (d); evaporation at oven (e); granulated and sieved samples (f); hot press (g); samples after pressing (h); analysis samples (i), TS analysis (k)

Characterization

Physical characterization

The interaction of PS composites with water is particularly important. For the physical characterization of the composite with the addition of pine and poplar fiber residues, 2 h (TSW2h) and 24 h (TSW24h) thickness swelling (TSW) and water absorption (WA) analyses were performed in accordance with the related ASTM standards. The samples were immersed in distilled water for 2 to 24 h. Samples with dimensions of 130 mm × 13 mm × 3.2 mm were prepared from each formulation, and 7 replicates were made for each group for statistical reliability. Analyses were carried out according to ASTM D1037 (2020) for WA, TSW2h and TSW24h, and ASTM D7032-21 (2021) for density measurement. Before the tests, the samples were conditioned at 20±2 °C and 65±5% relative humidity for 48 h. To evaluate short- and long term behavior, the samples were immersed in distilled water at 20 °C for TSW2h and TSW24h. Initial and final thicknesses (t_0 and t_1) and weights (W_0 and W_1) were measured, and WA and TSW were calculated using the Eqs. 1 and 2,

$$WA\ (\%) = \frac{W_1 - W_0}{W_0}\ x\ 100 \quad (1)$$

where W_0 is the initial dry weight (g) and W_1 is the weight after immersion (g).

$$TS2h\ or\ TS24h\ (\%) = \frac{T_1 - T_0}{T_0}\ x\ 100 \quad (2)$$

where T_0 is the initial thickness (mm) and T_1 is the thickness after immersion (mm).

Density (ρ) was calculated based on the mass to volume ratio of the conditioned samples as Eq. 3.

$$\rho\ (g/cm^3) = \frac{W_0}{V_0}\ x\ 100 \quad (3)$$

where W_0 is the initial dry weight (g) and V_0 is the initial volume (cm^3), calculated as length x width x thickness.

Mechanical characterization

For the mechanical characterization of the samples, tensile strength (TS), tensile modulus (TM), flexural strength (FS), flexural modulus (FM), and elongation at break (EatB) analyses were performed on the samples. The samples were first kept in a climate chamber at 20 °C and 65% relative humidity for 24 hr. Flexural tests were performed using a Zwick/Roell Z010 (ZwickRoell GmbH & Co. KG, Ulm, Germany) 5 kN testing machine according to ASTM D790-03 (2017), and tensile tests were performed according to ASTM D638-14 (2014) standards. The test speed for all tests was 3 mm/min. Seven replicates were performed for all formulations and their averages were used in this study.

Morphological characterization

Scanning electron microscopy (SEM) analysis was performed to examine the distribution of filler fiber residues in the PS matrix and whether they formed clusters. SEM was used to determine the morphological properties of the samples. Tescan MAIA3 XMU-SEM (Tescan Group, headquartered in Brno, Czech Republic) device was used for measurements. Measurements were made under 5 kV increasing voltage. The surface of the samples was coated with Denton spray to increase the surface conductivity.

Structural characterization

X-ray diffraction analysis (XRD) was performed to determine the structural characterization of the composites. XRD was performed with a Philips Panalytical Empyrean X-ray diffraction meter (Malvern Panalytical Ltd., headquartered in Almelo, Netherlands) using Ni-filtered Cu Kα (1.540562Å) radiation. The composites were scanned in the range of 10° to 80° 2θ, and the crystallinity of the samples was calculated using the Segal and curve fitting methods given in Eq. 4,

$$Crystallinity\ (\%) = \Sigma A_c/(\Sigma\ (A_a + A_c))\ x100 \quad (4)$$

where A_c is the integrated area under the respective crystalline peaks and A_a is the integrated area of the amorphous state.

Fourier transform infrared spectroscopy (FTIR)

Fourier transform infrared spectrophotometry (FTIR) analysis was performed to determine the changes in the chemical structure of the obtained composites with the addition of pine and poplar fiber residues to the recycled PS. FTIR analysis was performed with a Shimadzu IRAffinity-1 spectrometer (Shimadzu Corporation, headquartered in Kyoto, Japan) in the wavelength range of 700 to 4000 cm^{-1} at a resolution of 2 cm^{-1}. The average of five replicates were used for the samples in the study.

Statistical analysis

Statistical analysis was performed using SPSS 23 software (IBM Corp., Armonk, NY, USA) and one way analysis of variance (ANOVA) to determine whether there was a significant difference between the samples. The Duncan Post hoc test was used to determine how the various groups differed from each other.

RESULTS AND DISCUSSION

Physical Properties

The physical properties of PS composites with pine and poplar fiber residues additions are given in Table 4. According to the analysis results, it was determined that the samples left in water for TSW2h and TSW24h swelled by 0.37 to 1.65% and 0.75 to 4.93%, respectively. Also, pine and poplar fiber residue addition increased the water absorption of the composites by 0.28% to 2.3% and 0.36 to 9.52% for WA2h and WA24h, respectively. In the literature, the density of neat polystyrene is reported as 1000 to 1060 kg/m^3 (Yourtee and Cooper 1974). When Fig. 2a is examined, it is seen that the density of recycled neat PS was close to these values. It is understood that in neat PS, the solvent acetone was largely removed in the oven. A small amount of solvent was trapped in the matrix. This was detected by voids in the SEM images.

Table 4. Physical Result of Samples

Samples	TSW2h (%)	TSW24h (%)	WA2h (%)	WA24h (%)	Density (kg/m^3)
Neat PS	0.37 (±0.33)* A**	0.75 (±1.4) AB	0.28 (±0.26) A	0.36 (±0.24) A	1004 (±3.3) B
10%Pine	1.09 (±0.76) AB	2.3 (±1.0) B	1.07 (±0.31) C	4.86 (±1.8) C	1071 (±56) C
20%Pine	1.65 (±0.46) B	3.55 (±0.69) C	1.84 (±0.36) D	8.43 (±1.2) D	1009 (±33) B
30%Pine	1.64 (±1.15) B	4.93 (±1.9) D	2.3 (±0.25) E	9.52 (±1.02) C	1036 (±72) BC
10%Poplar	0.37 (±0.23) A	1.37 (±0.98) AB	0.58 (±0.22) B	1.68 (±0.73) B	1020 (±58) BC
20%Poplar	0.82 (±0.5) AB	1.85 (±0.61) A	1.4 (±0.05) AB	2.95 (±0.58) B	851 (±72) A
30%Poplar	1.37 (±1.20) B	2.64 (±0.47) A	2.15 (±0.19) A	3.52 (±0.18) A	979 (±15) B

* Standard deviation
** Duncan analysis, homogeneous subsets. Values within a column followed by different letters are significantly different at $p < 0.05$ according to Duncan's multiple range test

The addition of pine fiber residue generally increased the density of the PS composite. In the literature, the density of solid pine wood is reported as 508 kg/m^3 (Bal and Ayata 2020; Chin *et al.* 2023). However, this density can be attributed to a porous (with air) structure. Since the pine fiber residue used in the study was milled, these voids were eliminated, leaving behind solid pine.

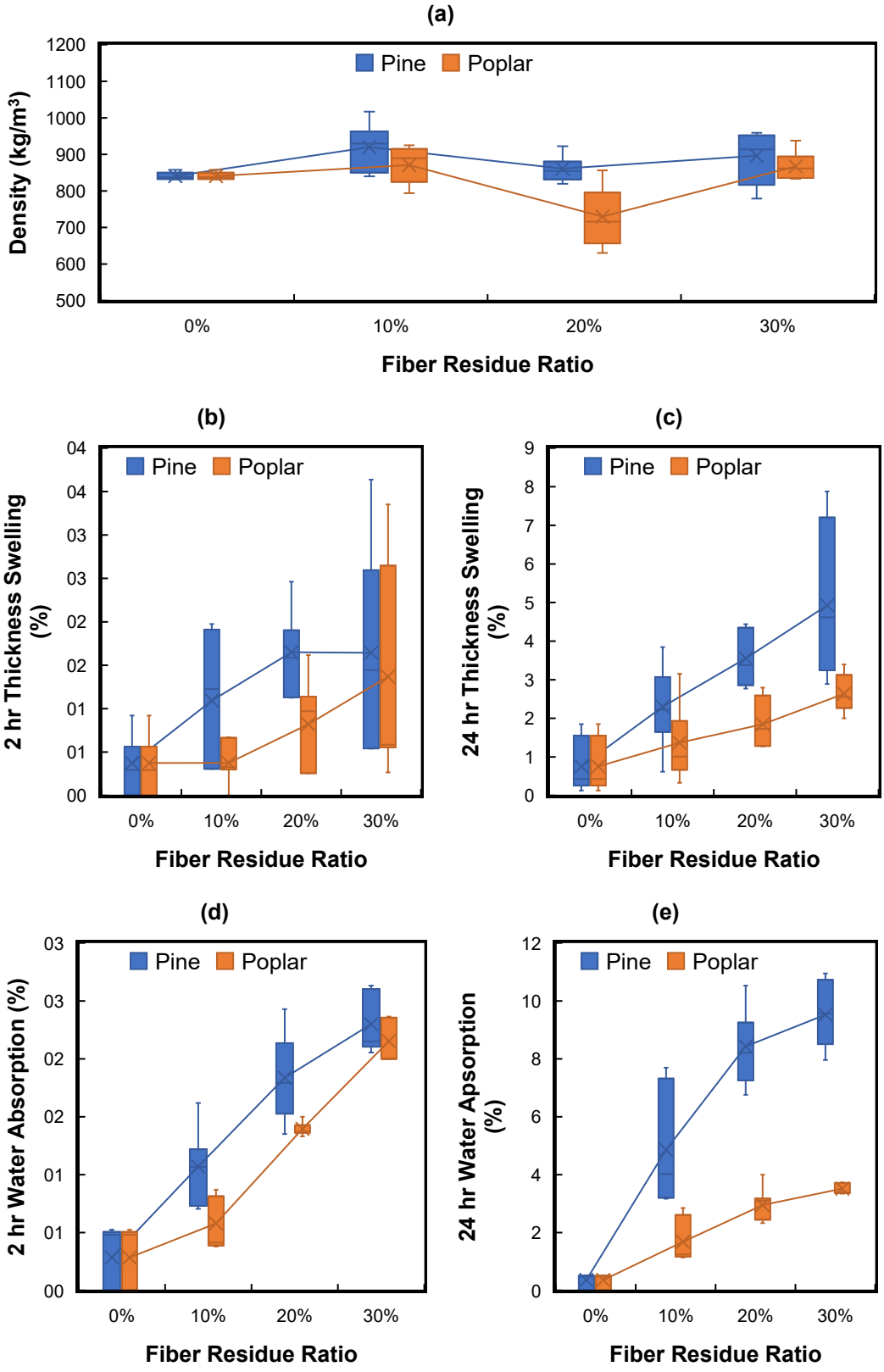

Fig. 2. Density (a), TSW2h (b), TSW24h (c), WA2h (d) and WA24h (e) results of the samples

It is reported that the cell wall wood density of solid pine and poplar is approximately 1500 kg/m^3 (Björklund *et al.* 2021; Chin *et al.* 2023). When considered from this perspective, if there is no air void in the fiber residue added to PS, it will increase the density of PS.

It is apparent that the densities were lower than the control sample only in poplar 20% and 30% samples (Fig. 2a). The addition of 10% poplar did not cause a significant change in the density of the composite. However, the addition of 20% and 30% poplar significantly reduced the density of the composite (2 to 15%). The density decreased as the poplar fiber residue content increased. To more clearly interpret the density decrease, it is necessary to determine how additions of 30% or more affect the densities. In the latter case, the addition of 10% poplar fiber residue did not change the PS density, while the density decreased as the filler ratio increased. The decrease in density in the samples appears to be due to the poplar forming a more foam-like structure in the matrix rather than to the incompatibility of the matrix poplar interface. The increase in mechanical strength as the poplar fiber residue increases supports this hypothesis.

According to the TSW2h and TSW24h results, a significant increase in the swelling tendency was observed in pine fiber residue added samples as the ratio increased (Fig. 2b). In the 30% pine, the swelling ratio reached 4.93% at the end of 24 hr (Fig. 2c). In poplar fiber residue added composites, the swelling was more limited at all ratios (max. ~3.52%). Poplar fiber residues both reduced the density of the composite and exhibited lower TSW2h, TSW24h, and WA2h WA24h compared to pine fiber residues. It is known in the literature that poplar (*Populus* spp.) fibers generally contain higher hemicellulose than pine (*Pinus* spp.) fibers (Fengel and Wegener 1984; Hon and Shiraishi 2001; Rowell 2005). However, the fibers used in this study were residue fibers obtained after lignin extraction, and a significant portion of the hemicellulose can dissolve and be removed during the extraction process. Poplar fibers, with a hemicellulose content predominantly dominated by xylan, tend to become more soluble during extraction processes and experience greater losses (Ma *et al.* 2015). In contrast, because the galactoglucomannan type hemicelluloses found in pine fibers are more resistant to extraction, relatively higher hemicellulose residues may be present in pine fibers after processing (Price *et al.* 2011). This can be considered a possible explanation for the lower than expected water absorption behavior of the poplar reinforced composites in the present study and the difference compared to the pine-reinforced composites.

2 hr WA for pine and poplar were close to each other (Fig. 2d). However, at 24 hr WA the difference widened and pine absorbed more water than poplar. The WA2h and WA24h results of the samples also showed a similar trend. While the water absorption approached 10% in 30%Pine sample at the end of 24 hr, this value remained below 4% in poplar fiber residue added samples (Fig. 2e).

The Grubbs test ($\alpha = 0.05$) was applied to identify potential outliers in the data set. Analyses were performed separately for each group and measurement parameter (TSW2h, TSW24h, WA2h, WA24h, and Density). The Grubbs statistic values obtained were above the calculated critical values, and no statistically significant outliers were detected in any group. This result demonstrates that all measurements exhibited homogeneous distributions and could be used confidently in statistical analyses.

Mechanical Properties

The mechanical strength analysis results of PS composite samples are given in Table 5. According to the results, the type and ratio of additives played a decisive role in

the mechanical performance of the PS matrix. The neat PS sample had the lowest TS of approximately 6.5 MPa. This situation shows that PS, which exhibits a brittle structure, has limited resistance capacity under external loads. The use of lignocellulosic reinforcement was implemented to overcome this limitation.

Table 5. Mechanical Properties of Reinforced PS Samples

Samples	TS (MPa)	TM (MPa)	FS (MPa)	FM (MPa)	EatB (%)
Neat PS	6 (±1.1) * A**	2343 (±182) D	18.2 (±2.7) A	955 (±134) BC	2.74 (±0.3) A
10%Pine	16 (±2.5) C	986 (±28) B	33.1 (±4.3) D	1135 (±172) C	5.82 (±0.4) CD
20%Pine	12.8 (±2.3) B	639 (±119) A	31.1 (±3.9) CD	1033 (±146) BC	5.3 (±0.7) C
30%Pine	12.6 (±1.5) B	1091(±77) B	27.7 (±2.0) BC	972 (±174) BC	5.2 (±1.2) C
10%Poplar	8.7 (±1.2) A	635 (±42) A	26.3 (±0.6) B	923 (±106) B	6.4 (±0.9) D
20%Poplar	11.9 (±2.9) B	1294 (±66) C	26.6 (±0.8) B	644 (±128) A	4.1 (±0.7) B
30%Poplar	14.5 (±3.3) BC	2347 (±232) D	29.6 (±2.9)BCD	842 (±151) B	3.8 (±0.5) B

* Standard deviation
** Duncan analysis, homogeneous subsets, Values within a column followed by different letters are significantly different at $p < 0.05$ according to Duncan's multiple range test

In the composites prepared with the addition of pine fiber residue, the highest TS was obtained with a value of approximately 18 MPa obtained at a 10% filling level (Fig. 3a). This increase shows that the low level of pine filling provided a homogeneous distribution within the PS matrix and that the matrix interaction was strong. However, when the filling ratio was increased to 20% and 30%, a decrease in TS was observed (~14 MPa and ~13 MPa, respectively). This decrease can be explained by the fact that the high fiber residue content creates agglomeration in the matrix, increases the void volume and causes weaknesses in stress transfer for pine fiber residues. In addition, it is thought that the matrix interface bond weakens at high pine fiber residue filler ratios.

In poplar fiber residue added samples, the TS obtained at 10% filling ratio remained at the level of ~9 MPa and provided a limited improvement. On the other hand, significant increases were observed at 20% and 30% filling ratios and strength values of approximately 13 and 15.5 MPa were reached, respectively. This finding shows that poplar fiber residues exhibited better interface compatibility with PS and could maintain structural integrity even at high ratios. The particle size, surface energy and morphological properties of poplar fiber residues may have provided a more compatible distribution and bonding with the PS matrix.

According to the TM analysis result, it is apparent that the elasticity of neat PS was the highest (Fig. 3b). The addition of pine and poplar fiber residue reduced the elasticity of the specimens. Pine fiber residues reduced elasticity more than poplar fiber residues. As the addition of poplar increased, elasticity increased. While neat polystyrene exhibits high elasticity, the decrease in elasticity at 10% filler addition and the increase again at higher filler ratios can be explained by microstructural changes. At low filler levels, the uneven distribution of particles in the matrix may have led to stress concentrations and void formation (Sahai and Pardeshi 2021). At higher filler ratios, increased interparticle contact may have increased the load carrying capacity and led to a more rigid matrix structure (Aksit *et al.* 2019; Gwóźdź-Lasoń *et al.* 2025).

Wood fiber residue was found to reduce the TM of the PS composite, which is undesirable in composites. However, the purpose of the fiber addition was not solely to increase the modulus; the study aimed to improve other mechanical properties, particularly

tensile strength (TS) and flexural strength (FS), and to evaluate the environmental advantages of biofiber additions. Indeed, while the tensile strength of neat PS was 6 MPa, it increased to 16 MPa with 10% pine reinforcement and to 14.5 MPa with 30% poplar reinforcement, and flexural strength increased to 33.1 MPa. Duncan's multiple comparison test results indicated statistically significant differences in these properties between neat PS and reinforced samples ($p < 0.05$).

Therefore, the primary objective of the study was not merely to increase stiffness, but to reveal the multidimensional effects and ecological benefits of fiber addition on mechanical performance.

Overall, maximum TS was obtained with 10% pine fiber residue additive; However, this type of additive had a negative effect on the mechanical properties at high rates. On the other hand, the poplar fiber residue filling, especially when used at 30%, increased the strength value and supported structural rigidity. These results show that the mechanical properties of recycled PS based composites can be improved, provided that residue lignocellulosic fibers are used at appropriate rates.

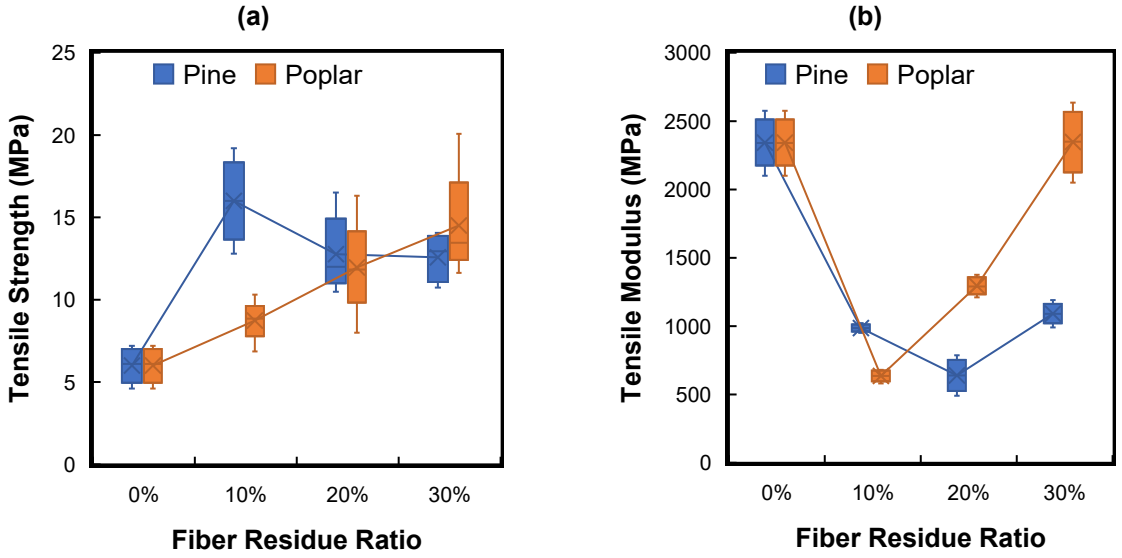

Fig. 3. TS (a) and TM (b) of samples

It is shown that the fiber type and ratio significantly affected the FS and FM behaviors of the composites. According to the FS results, a significant strength increase was observed in the pine fiber residue-filled samples at 10% and 20% (Fig. 4a). However, a decrease was observed in FS when the filler ratio increased to 30%, compared to neat polystyrene. This situation can be explained by the reinforcement effect of the pine fiber residues at low ratios by supporting the load transfer in the matrix. High ratio pine fiber residue addition caused weak interface with the matrix. When there are clusters of fibers, there may have been insufficient wetting of their surfaces by the resin, leading to a point of weakness in the structure. Thus, it caused the deterioration of stress transfer and decreased mechanical performance (Alias *et al.* 2021). In a similar study, the mechanical properties of wood plastic composites produced using different proportions of recycled plastic and acacia wood fiber were investigated and it was reported that both tensile and flexural strengths increased significantly as the plastic ratio increased (Gulitah and Liew 2018). Similar trends have been reported in the literature; Ashori and Nourbakhsh (2009)

stated that mechanical strength decreased with increasing fiber ratio in wood fiber composites produced from recycled plastics due to interfacial incompatibility. Similarly, Sihombing *et al.* (2012) stated that the inhomogeneous distribution of fibers within the matrix and hydrophobic hydrophilic incompatibility were among the main factors limiting the mechanical properties of wood plastic composites obtained from recycled materials.

In poplar fiber residue added composites (10%Poplar sample), the FS remained at lower levels compared to pine. However, as the filler ratio increased, FS increased linearly, unlike the pine fiber residue filler. Kaseem *et al.* (2017) reported similar results in their study. The addition of poplar fiber linearly increased the FS strength of the polystyrene composite. This increase continued to a 30% filler ratio, after which it began to decrease. In the sample with 20% poplar fiber residue addition, the density decreased excessively, and this decrease caused the FS and FM to decrease (Fig. 4b).

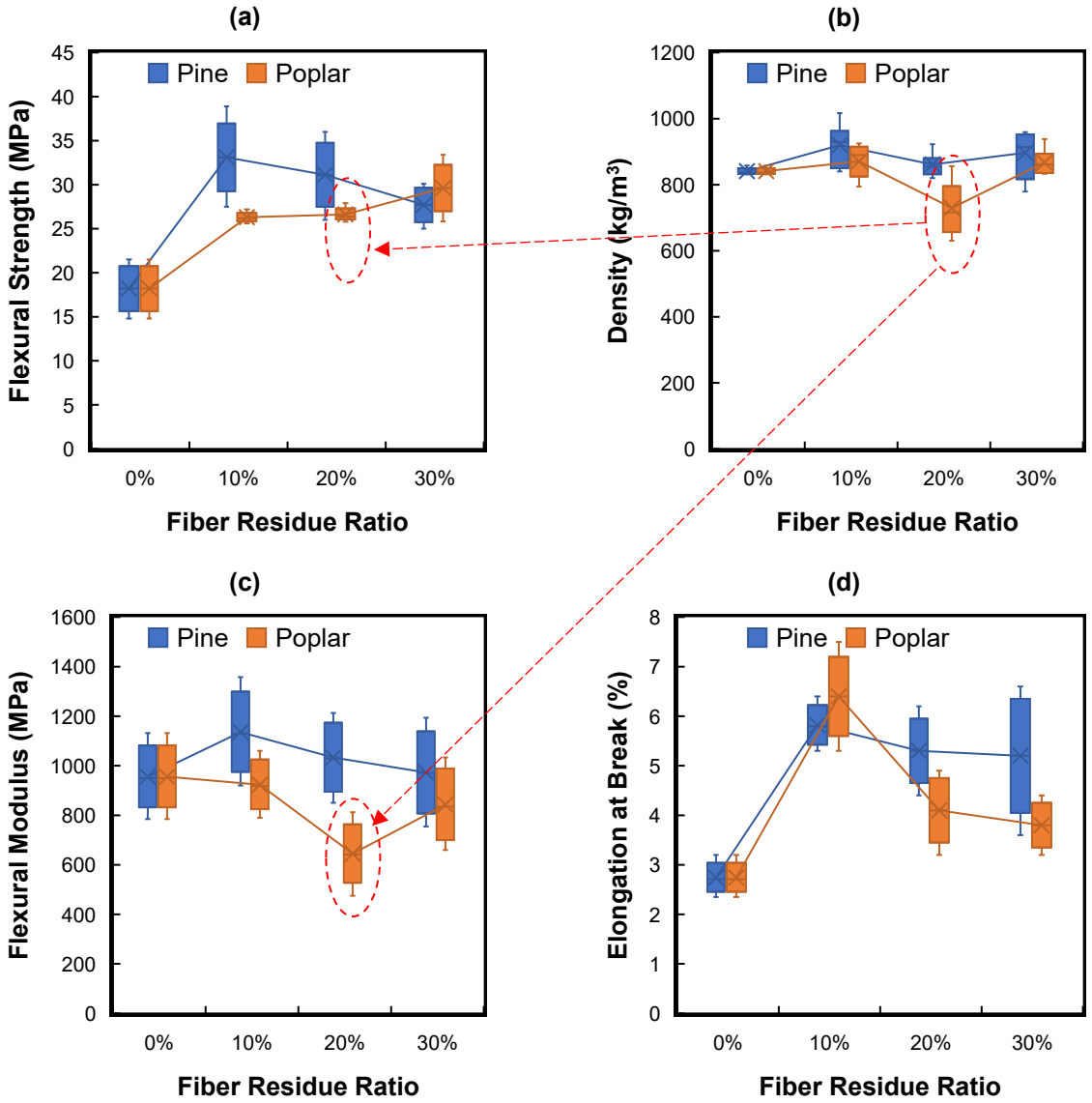

Fig. 4. FS (a); density (b); FM (c); and EatB (d) of samples

FM results reveal the effect of pine and poplar filling differently (Fig. 4c). In pine-filled samples, the FM value decreased as the filling ratio increased. This indicates that a high percentage of pine fiber residues reduces stress distribution within the matrix and reduces the load carrying capacity of the sample (Yuan *et al.* 2025). On the other hand, the FM value in poplar added composites decreased as the additive ratio increased. This remarkable result can be explained by the low stress distribution of poplar fiber residues in the PS matrix (Lisperguer *et al.* 2011). In addition, the fact that poplar fiber residues are dimensionally thinner and more flexible may have had a negative effect on the modulus. It has been stated in the literature that low density, but well oriented fiber residues can increase the flexural modulus (Rowell 2012).

When the density data and FS result were evaluated together, it was observed that low density poplar filled samples offered a more stable structure, in terms of FM. In pine filled samples, although high FS can be achieved with high density, this effect was only valid at low filling ratios.

The EatB results given in Fig. 4d provide evidence about the ductility character of the samples. While the Neat PS sample exhibited the most brittle structure with the lowest EatB value (~3%), the EatB value in pine fiber residue filled composites increased up to 6–7% at 10% and 30%. This increase shows that the fiber residues contributed to the plastic deformation process and absorbed energy at the moment of fracture (Bollakayala *et al.* 2022). The EatB value in poplar fiber residue filled composites is lower than that of pine (John and Thomas 2008). This indicates that poplar fiber residues limit the deformation time by behaving more rigidly. This rigid structure also occurred in the WA24h and TSW24h structures of the samples. The ductility of the poplar fiber residue added PS matrix decreased and reduced the effects of water.

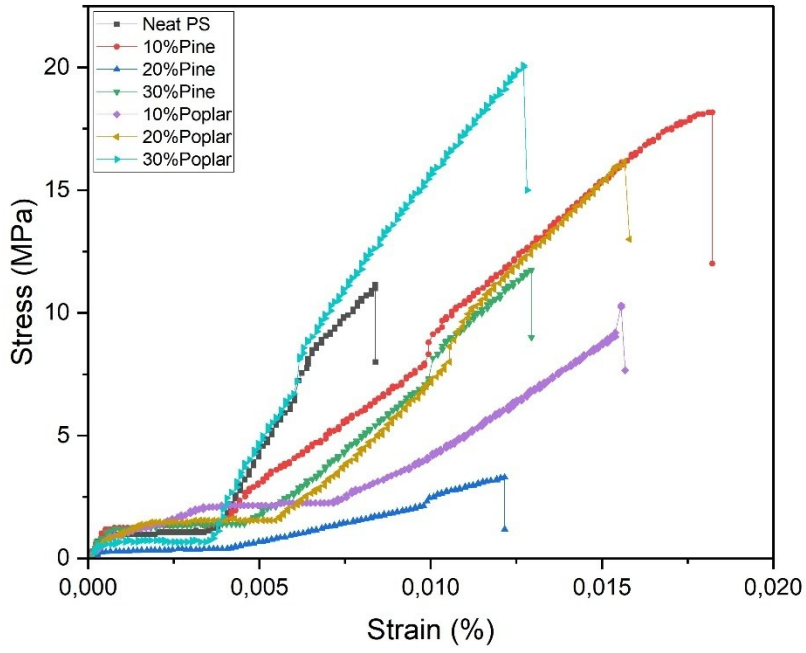

Fig. 5. Stress and strain graphic of pine and poplar added samples

The stress strain curves in Fig. 5 show the mechanical deformation behaviors of PS composites containing pine and poplar fiber residues at different ratios. While the neat PS sample was characterized by low deformation capacity and sudden fracture, the 10% and

30% pine added samples especially exhibited higher fracture strain and maximum stress. This shows that the fiber residues contributed to energy absorption in the matrix and increased ductility. The most remarkable result in the poplar filled samples was obtained at 30% additive ratio; this sample reached the highest stress value of approximately 20 MPa. This shows that the poplar fiber residues were better integrated into the matrix and contributed effectively to the load carrying capacity. The fiber type and ratio directly affected the deformation mode of the composites, especially the high ratio filling improved ductility and strength (Bandelt and Billington 2016).

SEM Analysis Results

The morphological properties of the fracture surfaces of neat PS and pine (10-20-30%) added samples are given in Fig. 6. Figure 6(a) shows that with the neat PS sample, there was no fiber residue phase on the surface. Instead, distinct saw marks formed (trace) during the cutting of the samples. This structure indicates a homogeneous matrix structure, and no voids or matrix interaction were observed because of gas release. This shows that the acetone solvent was completely removed in Neat PS.

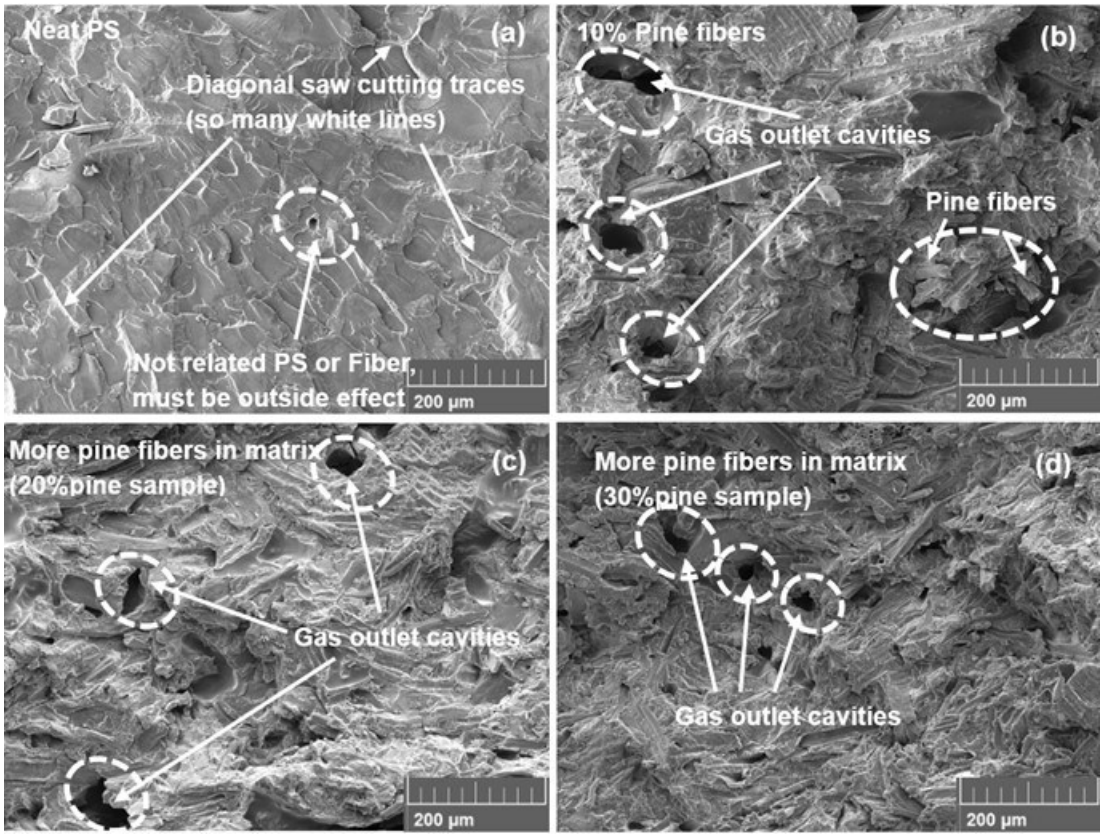

Fig. 6. Pine fiber residue added samples SEM analysis results; Neat PS (a); 10%Pine (b); 20%Pine (c); 30%Pine (d)

When Fig. 6(b) is examined at 10%, it is apparent that the pine fiber residues were embedded in the matrix, but the matrix bond was weak in some areas and micro voids formed because gas release occurred. This situation showed that the solvent remained embedded in the matrix, albeit in small amounts. The dispersed structure of the fiber residues in the matrix indicates a homogeneous mixture. It is understood that the addition

of pine fiber residue contributes to the internal bonding strength of the matrix (with an increase of approximately 130% in TS strength).

In Fig. 6(c), it is shown that the fiber residues had increased and the fiber residues were more homogeneously distributed in the matrix. However, with increasing fiber residue ratio, the number and diameter of gas outlet cavities also increased. This situation caused a decrease in both sample density (-7%) and TS strength (-20%). When the pine fiber filling ratio increased to 30% (Fig. 6d), an insignificant decrease in density (-3%) and TS strength (-2%) was observed. Similar results were also experienced in FS strength.

In the sample containing 30% pine fiber residue, the presence of fiber residues in the matrix increased. This situation shows that high fiber residue content can negatively affect structural integrity by disrupting the continuity of the matrix. The increase in pine fiber residue content significantly affected the morphology of the composite structure; especially, it resulted in the weakening of matrix interface interactions and increased void formations (Saeed *et al.* 2021). This situation caused a decrease in TS and FS strength and density.

SEM images of samples with poplar fiber residue filling are given in Fig. 7. The black spot in Fig. 7a was not related to fiber residue or PS matrix. It may have been caused by an external impact. Quite large voids are visible in Fig. 7b. As the fiber residue ratio increased (from 10% to 20%), the diameter of the voids decreased. In the samples where poplar fiber residues were used, the microstructure development was more regular.

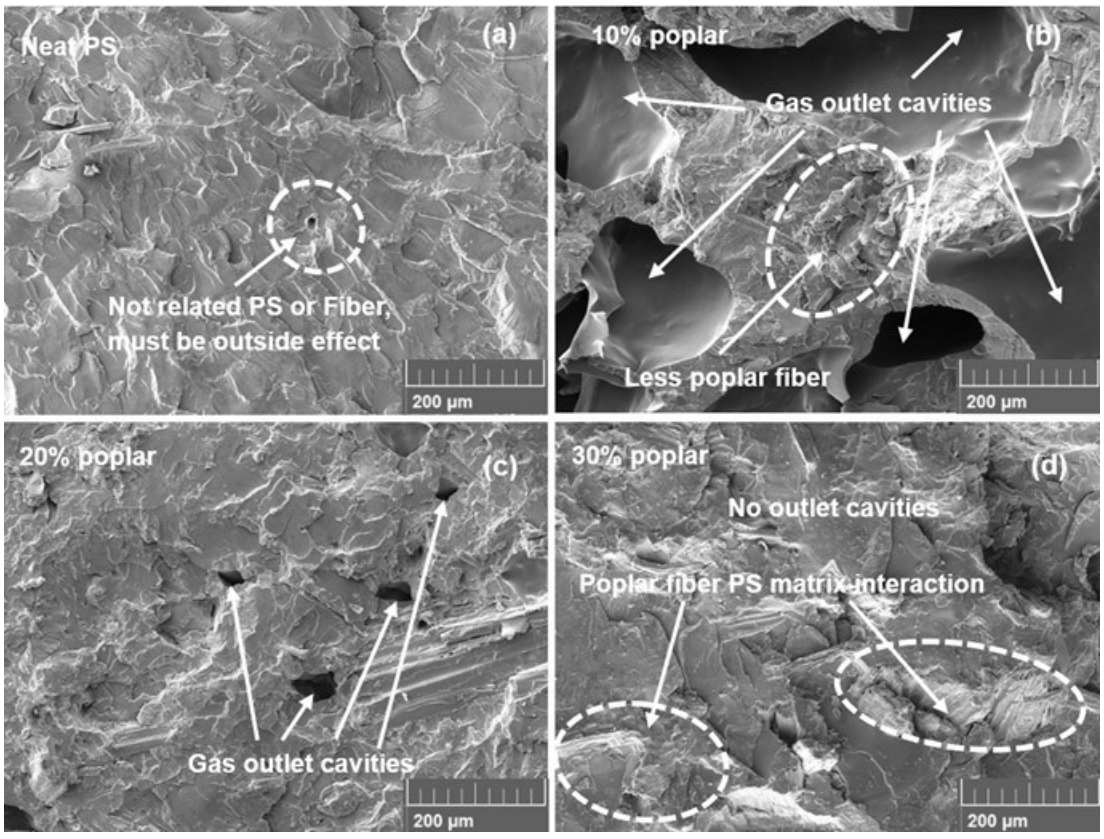

Fig. 7. Poplar fiber residue added samples SEM analysis, Neat PS (a); 10% Poplar (b); 20% Poplar (c); 30% Poplar (d)

In the sample with 20% poplar (Fig. 7c) and 30%poplar addition (Fig. 7d), the void free compact structure and the developed matrix interface became apparent. As a result of

this situation, FS and TS strength were kept higher than the pine filling (as the filler ratio increased) (FS ≈ 27 MPa, TS ≈ 15 MPa). The EatB value increased to 7%, showing a significant increase in plastic deformation ability (Fig. 4d). The addition of poplar fiber residue caused a decrease in density (~16%).

These results show that the surface properties and dimensional compatibility of poplar fiber residues led to better interfacial interaction with the PS matrix, thus providing a more stable and high performance structure.

XRD Results

All samples gave peaks around 19° to 22° 2θ (Fig. 8a). This generally shows that the pattern of the samples were similar to each other. Neat PS exhibited typical amorphous characteristics, with a broad, low intensity peak observed around 19–20° 2θ (Sun *et al* 2003; Huang *et al.* 2020) (Fig. 8b). This broad peak represents the irregular packing of the polystyrene chains and the low degree of crystallinity (Wichai and Vao-soongnern 2021).

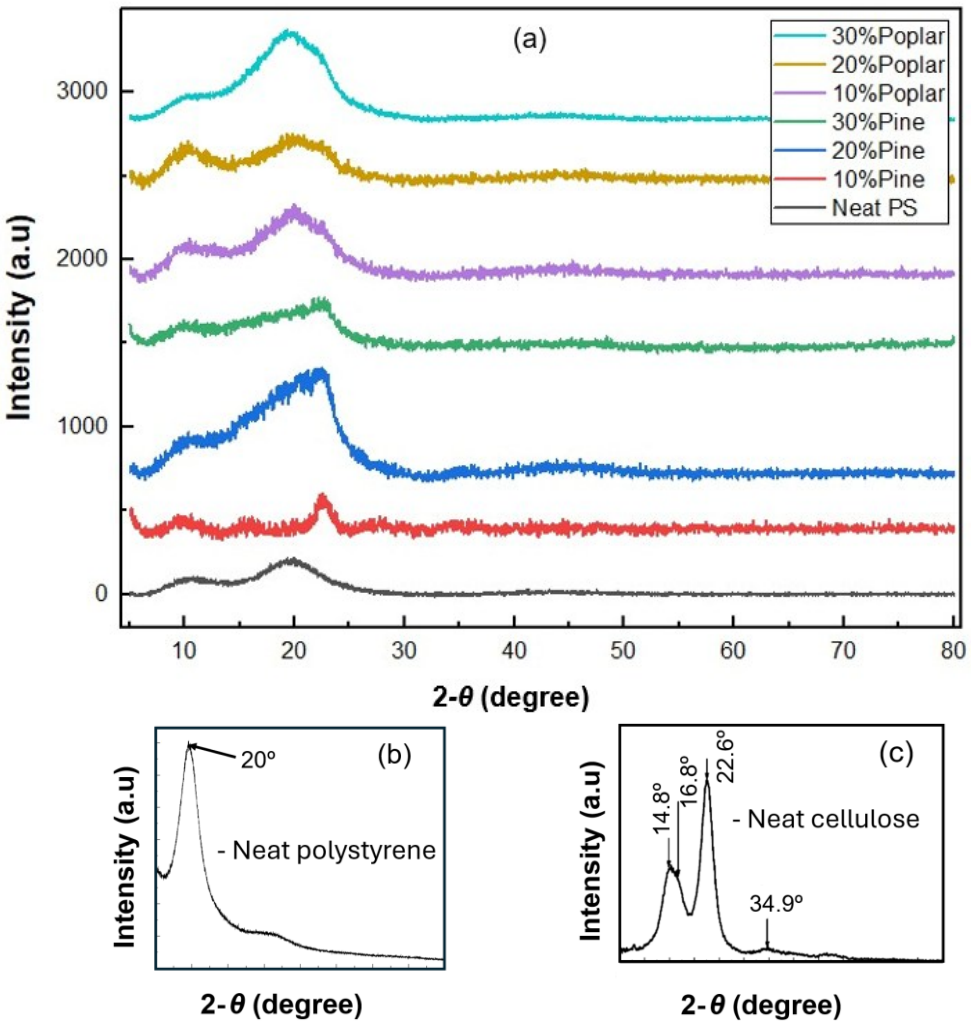

Fig. 8. XRD results of pine and poplar fiber residue filled samples (a), Neat PS (Huang *et al.* 2020) (b), and cellulose (c) (Mao *et al.* 2017)

Some changes in the patterns were observed in the samples with fiber residue reinforcement. The poplar fiber residue reinforced samples exhibited somewhat sharper and higher peak intensities compared to neat PS and pine fiber residue reinforced samples. Because cellulose is semi crystalline, the poplar addition increased the crystalline regions of the matrix, creating little higher peaks in the XRD patterns. This is attributed to the slightly higher cellulose content of the angiosperm-derived poplar fibers than the gymnosperm-derived pine fibers (Wang *et al.* 2020).

FTIR Results

The chemical effects of pine and poplar fiber residues added to the PS matrix on the composite structures are given by FTIR analysis (Fig. 9). Aromatic C–H stretching vibrations, indicating aromatic ring structures specific to polystyrene, were in the range of 3000 to 3100 cm^{-1}. These peaks were clearly present in all samples. CH_2 stretching vibrations of polystyrene were in the range of 2850 to 2920 cm^{-1}, aromatic ring modes vibrations were between 1600 and 1490 cm^{-1}, and aromatic ring bendings were in the range of 750 to 700 cm^{-1} (Yabagi *et al.* 2018). The characteristic glucose ring vibrations of the cellulose structure from pine and poplar fiber residues were around 1100 cm^{-1}, and the C–O vibrations, indicating cellulose and hemicellulose components, were in the band range of 1000 to 1200 cm^{-1} (Cherednichenko *et al.* 2022). The intensity of these peaks increased as the fiber ratio increased. The intensity of the peaks in the pine fiber residue reinforcement was not as pronounced as in poplar. However, they together give signals in similar regions. No distinct peaks indicating new functional groups were observed, indicating that no detectable amounts of covalent bonds were formed between the PS matrix and the fibers, but rather a physical mixture.

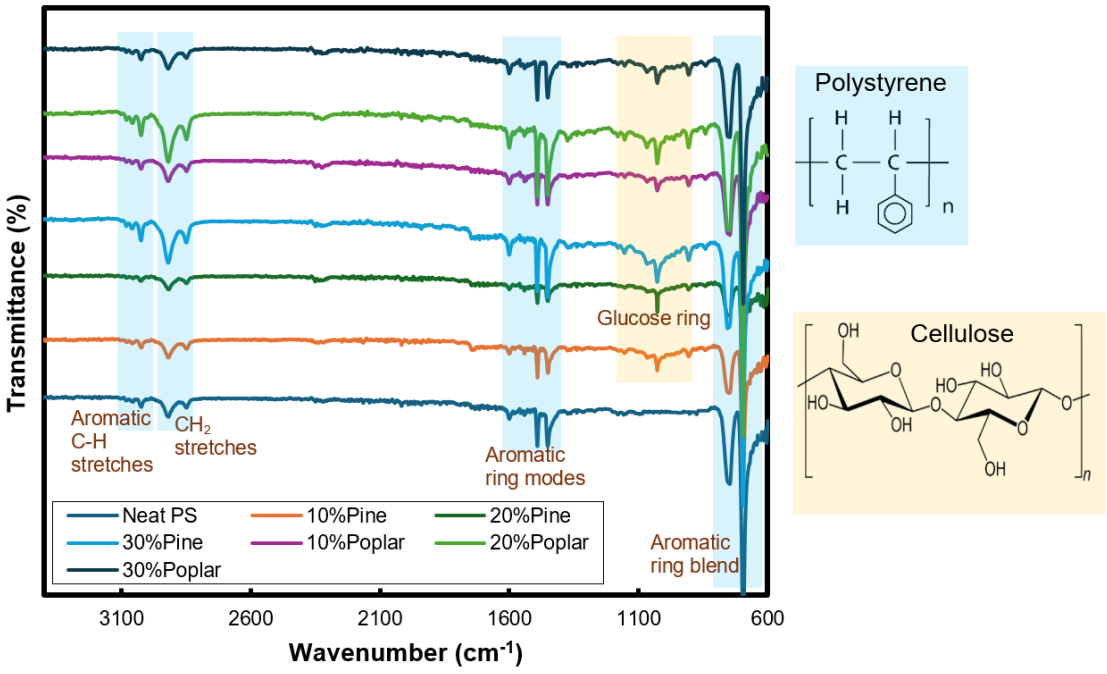

Fig. 9. FTIR analysis results

This study investigated the reinforcing effects of pine and poplar fibers (residual from lignin extraction) in recycled polystyrene matrix composites. However, due to the production method used and the high elastic modulus of the neat matrix, limited improvements were achieved in some mechanical properties. Future studies are recommended to strengthen the fiber-matrix interfacial bond by adding compatibilizing agents (*e.g.*, maleic anhydride polypropylene – MAPP, or similar agents). This may allow for more significant increases in mechanical properties.

Furthermore, optimizing the use of not only PS and compatibilizers but also plasticizers can reduce the excessive brittleness of the composite and improve toughness properties such as elongation at fracture. Such studies will provide the opportunity to evaluate the simultaneous effects of both fiber reinforcement and matrix modification and contribute to the development of environmentally sustainable, mechanically stable composites.

CONCLUSIONS

This study investigated the characteristics of fibers remaining after lignin extraction from pine and poplar wood within the recycled polystyrene (PS) matrix. The aim was to recycle forest and plastic industry residue (wood fiber residue and recycled polystyrene) by utilizing them in the production of wood-plastic composites.

1. Pine fiber residue filling increased PS density, while poplar fiber residue filling decreased (except 10%Poplar sample) the density.
2. Fiber residue addition increased PS composite water absorption (WA24h: ~1.9) and accordingly increased its swelling (~5.1%). Poplar fiber residue filling (TSW24h: ~1.6%) showed more resistance to swelling than pine fiber residue (TSW24h: ~8.7%) filling.
3. Pine and poplar fiber residues increased thickness swelling (TS) but decreased the tensile modulus (TM). The TS decreased as the pine fiber residue addition ratio increased. However, the TS increased as the poplar filling ratio increased. Similar results were obtained in flexural strength (FS) and flexural modulus (FM).
4. Fiber residues increased elongation at break (EatB) value in all samples. EatB decreased as fiber residue ratio increased.
5. It was determined in SEM images that acetone could not be completely removed due to the presence of fiber residues. Acetone under heat and pressure caused voids in the matrix.

REFERENCES CITED

Aksit, M., Zhao, C., Klose, B., Kreger, K., Schmidt, H.-W., and Altstädt, V. (2019). "Extruded polystyrene foams with enhanced insulation and mechanical properties by a benzene-trisamide-based additive," *Polymers* 11(2), article 268. DOI: 10.3390/polym11020268

Alias, A. H., Norizan, M. N., Sabaruddin, F. A., Asyraf, M. R. M., Norrrahim, M. N. F., Ilyas, A. R., Kuzmin, A. M., Rayung, M., Shazleen, S. S., Nazrin, A., Sherwani, S. F. K., Harussani, M. M., Atikah, M. S. N., Ishak, M. R., Sapuan, S. M., and Khalina, A. (2021). "Hybridization of MMT/lignocellulosic fiber reinforced polymer nanocomposites for structural applications: A review," *Coatings* 11(11), article 1355. DOI: 10.3390/coatings11111355

Angel Flores-Hernandez, M., Guillermo Torres-Rendon, J., Maria Jimenez-Amezcua, R., Guadalupe Lomeli-Ramirez, M., Javier Fuentes-Talavera, F., Antonio Silva-Guzman, J., and Garcia Enriquez, S. (2017). "Studies on mechanical performance of wood-plastic composites: Polystyrene-*Eucalyptus globulus* Labill," *BioResources* 12(3), 6392-6404. DOI: 10.15376/biores.12.3.6392-6404

Ashori, A., and Nourbakhsh, A. (2009). "Characteristics of wood–fiber plastic composites made of recycled materials," *Waste Management* 29(4), 1291-1295. DOI: 10.1016/j.wasman.2008.09.012

ASTM D638. (2014). "Test method for tensile properties of plastics," *D638-14*, ASTM International, West Conshohocken, PA. DOI: 10.1520/D0638-14

ASTM D790. (2017). "Test methods for flexural properties of unreinforced and reinforced plastics and electrical insulating materials," *D20.10*, ASTM International, West Conshohocken, PA. DOI: 10.1520/D0790-17

ASTM D1037. (2020). *Test methods for evaluating properties of wood-base fiber and particle panel materials*, West Conshohocken, PA. DOI: 10.1520/D1037-12R20

ASTM D7032. (2021). *Specification for establishing performance ratings for wood-plastic composite and plastic lumber deck boards, stair treads, guards, and handrails*, West Conshohocken, PA. DOI: 10.1520/D7032-21

Bal, B. C., and Ayata, Ü. (2020). "Karaçam ve karakavak odunlarının bazı mekanik özellikleri üzerine karşılaştırmalı bir çalışma," *Türkiye Ormancılık Dergisi* 21(4), 461-467.

Bandelt, M. J., and Billington, S. L. (2016). "Impact of reinforcement ratio and loading type on the deformation capacity of high-performance fiber-reinforced cementitious composites reinforced with mild steel," *Journal of Structural Engineering* 142(10), article 1562. DOI: 10.1061/(ASCE)ST.1943-541X.0001562

Björklund, J., Fonti, M. V., Fonti, P., Van den Bulcke, J., and von Arx, G. (2021). "Cell wall dimensions reign supreme: Cell wall composition is irrelevant for the temperature signal of latewood density/blue intensity in Scots pine," *Dendrochronologia* 65, article 125785. DOI: 10.1016/j.dendro.2020.125785

Bollakayala, V. L., Etakula, N., Vuba, K. K., Manne, Y. S., and Uttaravalli, A. N. (2022). "Preparation and characterization of green composites based on expanded polystyrene waste and biomass: Sustainable management approach," *Materials Today: Proceedings*, 66, 1762-1768. DOI: 10.1016/j.matpr.2022.05.275

Calvin, K., Dasgupta, D., Krinner, G., Mukherji, A., Thorne, P. W., Trisos, C., Romero, J., Aldunce, P., Barret, K., Blanco, G., Cheung, W. W. L., Connors, S. L., Denton, F., Diongue-Niang, A., Dodman, D., Garschagen, M., Geden, O., Hayward, B., Jones, C., Jotzo, F., Krug, T., Lasco, R., Lee, Y.-Y., Masson-Delmotte, V., Meinshausen, M., Mintenbeck, K., Mokssit, A., Otto, F. E. L., Pathak, M., Pirani, A., Poloczanska, E., Pörtner, H.-O., Revi, A., Roberts, D. C., Roy, J., Ruane, A. C., Skea, J., Shukla, P. R., Slade, R., Slangen, A., Sokona, Y., Sörensson, A. A., Tignor, M., van Vuuren, D., Wei, Y.-M., Winkler, H., Zhai, P., Zommers, Z., Hourcade, J.-C., Johnson, F. X., Pachauri, S., Simpson, N. P., Singh, C., Thomas, A., Totin, E., Alegría, A., Armour,

K., Bednar-Friedl, B., Blok, K., Cissé, G., Dentener, F., Eriksen, S., Fischer, E., Garner, G., Guivarch, C., Haasnoot, M., Hansen, G., Hauser, M., Hawkins, E., Hermans, T., Kopp, R., Leprince-Ringuet, N., Lewis, J., Ley, D., Ludden, C., Niamir, L., Nicholls, Z., Some, S., Szopa, S., Trewin, B., van der Wijst, K.-I., Winter, G., Witting, M., Birt, A., and Ha, M. (2023). *IPCC, 2023: Climate Change 2023: Synthesis Report, Summary for Policymakers. Contribution of Working Groups I, II and III to the Sixth Assessment Report of the Intergovernmental Panel on Climate Change [Core Writing Team, H. Lee and J. Romero (eds.)]. IPCC, Geneva, Switzerland.*, Geneva, Switzerland. DOI: 10.59327/IPCC/AR6-9789291691647.001

Cherednichenko, K. A., Sayfutdinova, A. R., Kraynov, A., Anikushin, B., Ignatiev, V., Rubtsova, M. I., Konstantinova, S. A., Shchukin, D. G., and Vinokurov, V. A. (2022). "A rapid synthesis of nanofibrillar cellulose/polystyrene composite via ultrasonic treatment," *Ultrasonics Sonochemistry* 90, article 106180. DOI: 10.1016/j.ultsonch.2022.106180

Chin, Y. H., Biwole, P. H., Gril, J., Vial, C., Pitti, R. M., Ouldboukhitine, S. E., and Horikawa, Y. (2023). "Optimisation of alcoholysis treatment in Poplar wood delignification," in: *12èmes Journées Scientifiques du GDR 3544, Sciences du Bois*, Limoges, France, 251-254.

De-la-Torre, G. E., Dioses-Salinas, D. C., Pizarro-Ortega, C. I., and Saldaña-Serrano, M. (2020). "Global distribution of two polystyrene-derived contaminants in the marine environment: A review," *Marine Pollution Bulletin* 161, article 111729. DOI: 10.1016/j.marpolbul.2020.111729

ECHA. (2023). "Restriction proposal for intentionally added microplastics in the EU – update," *ECHA News*.

Eroğlu, Ö., Çetin, N. S., Narlıoğlu, N., and Yan, W. (2023). "Plastic/fiber composite using recycled polypropylene and fibers from *Sorghum halepense* L.," *BioResources* 18(2), 3109-3122. DOI: 10.15376/biores.18.2.3109-3122

European Commission. (2023). "Commission Regulation (EU) 2023/2055 of 25 September 2023 amending Annex XVII to Regulation (EC) No 1907/2006 of the European Parliament and of the Council concerning the Registration, Evaluation, Authorisation and Restriction of Chemicals (REACH) as regards synthetic polymer microparticles," *Official Journal of the European Union*.

Fengel, D., and Wegener, G. (1984). *Wood: Chemistry, Ultrastructure, Reactions*, Walter de Gruyter, Berlin, 613 pp.

De Frond, H., Thornton Hampton, L., Kotar, S., Gesulga, K., Matuch, C., Lao, W., Weisberg, S. B., Wong, C. S., and Rochman, C. M. (2022). "Monitoring microplastics in drinking water: An interlaboratory study to inform effective methods for quantifying and characterizing microplastics," *Chemosphere* 298, article 134282. DOI: 10.1016/j.chemosphere.2022.134282

García-Sobrino, R., Cortés, A., Calderón-Villajos, R., Díaz, J. G., and Muñoz, M. (2023). "Novel and accessible physical recycling for expanded polystyrene waste with the use of acetone as a solvent and additive manufacturing (direct ink-write 3D printing)," *Polymers* 15(19), article 3888. DOI: 10.3390/polym15193888

Gulitah, V., and Liew, K. C. (2018). "Effect of plastic content ratio on the mechanical properties of wood-plastic composite (WPC) made from three different recycled plastic and acacia fibres," *Transactions on Science and Technology* 5(2), 184-189.

Gündüz, İ. O. (2013). "Bir çevre vergisi türü olarak enerji vergisi: Fosil yakitlarin vergilendirilmesi-II," *Çukurova Üniversitesi Sosyal Bilimler Enstitüsü Dergisi* 22(2), 127-143.

Gwóźdź-Lasoń, M., Brachaczek, W., Kadela, M., and Kukiełka, A. (2025). "Physical properties of foamed concrete based on plaster mortar with polystyrene granulate and synthetic foaming agent," *Materials* 18(9), article 2115. DOI: 10.3390/ma18092115

Hon, D. N. S., and Shiraishi, N. (2001). "Wood and cellulosic chemistry," in: *Markel Decker*, Marcel Decker, USA, pp. 914-922.

Huang, G., Xu, J., Geng, P., and Li, J. (2020). "Carrier flotation of low-rank coal with polystyrene," *Minerals*, 10(5), 452. DOI: 10.3390/min10050452

John, M., and Thomas, S. (2008). "Biofibres and biocomposites," *Carbohydrate Polymers* 71(3), 343-364. DOI: 10.1016/j.carbpol.2007.05.040

Kaho, S. P., Kouadio, K. C., Kouakou, C. H., and Eméruwa, E. (2020). "Development of a composite material based on wood waste stabilized with recycled expanded polystyrene," *Open Journal of Composite Materials* 10(03), 66-76. DOI: 10.4236/ojcm.2020.103005

Kaseem, M., Hamad, K., Deri, F., and Ko, Y. G. (2017). "Effect of wood fibers on the rheological and mechanical properties of polystyrene/wood composites," *Journal of Wood Chemistry and Technology* 37(4), 251-260. DOI: 10.1080/02773813.2016.1272127

Köksal, S. E., and Kelleci, O. (2024). "Production and characterization of wood polystyrene composite from recycled waste materials," *Düzce Üniversitesi Orman Fakültesi Ormancılık Dergisi* 20(1), 375-394. DOI: 10.58816/duzceod.1453919

Kukharchyk, T. I., and Chernyk, V. D. (2022). "Soil pollution with microplastic in the impact area of a plant producing expanded polystyrene," *Eurasian Soil Science* 55(3), 377-386. DOI: 10.1134/S1064229322030085

Kwon, B. G., Koizumi, K., Chung, S.-Y., Kodera, Y., Kim, J.-O., and Saido, K. (2015). "Global styrene oligomers monitoring as new chemical contamination from polystyrene plastic marine pollution," *Journal of Hazardous Materials* 300, 359-367. DOI: 10.1016/j.jhazmat.2015.07.039

Lisperguer, J., Bustos, X., and Saravia, Y. (2011). "Thermal and mechanical properties of wood flour–polystyrene blends from postconsumer plastic waste," *Journal of Applied Polymer Science* 119(1), 443-451. DOI: 10.1002/app.32638

Ma, J., Ji, Z., Chen, J. C., Zhou, X., Kim, Y. S., and Xu, F. (2015). "The mechanism of xylans removal during hydrothermal pretreatment of poplar fibers investigated by immunogold labeling," *Planta* 242(1), 327-337. DOI: 10.1007/s00425-015-2313-5

Mao, R., Meng, N., Tu, W., and Peijs, T. (2017). "Toughening mechanisms in cellulose nanopaper: the contribution of amorphous regions," *Cellulose* 24(11), 4627-4639. DOI: 10.1007/s10570-017-1453-0

Milbrandt, A., Coney, K., Badgett, A., and Beckham, G. T. (2022). "Quantification and evaluation of plastic waste in the United States," *Resources, Conservation and Recycling* 183, article 106363. DOI: 10.1016/j.resconrec.2022.106363

Nair, K. M., Diwan, S. M., and Thomas, S. (1996). "Tensile properties of short sisal fiber reinforced polystyrene composites," *Journal of Applied Polymer Science* 60(9), 1483-1497.

Pollard, S. (1958). "Investment, consumption and the industrial revolution," *The Economic History Review* 11(2), article 215. DOI: 10.2307/2592317

Price, N. P., Hartman, T. M., Faber, T. A., Vermillion, K. E., and Fahey Jr, G. C. (2011). "Galactoglucomannan oligosaccharides (GGMO) from a molasses byproduct of pine (*Pinus taeda*) fiberboard production," *Journal of Agricultural and Food Chemistry*, 59(5), 1854-1861.

Rhodes, C. J. (2019). "Solving the plastic problem: From cradle to grave, to reincarnation," *Science Progress* 102(3), 218-248. DOI: 10.1177/0036850419867204

Rowell, R. (2005). "Cell Wall Chemistry," in: *Handbook of Wood Chemistry and Wood Composites*, R. M. Rowell and R. M. Rowell (eds.), CRC Press, Boca Raton, pp. 1-42. DOI: 10.1201/9780203492437

Rowell, R. (2012). "*Wood Thermoplastic Composites*," in: *Handbook of Wood Chemistry and Wood Composites*, R. M. Rowell and R. M. Rowell, eds., CRC Press, Boca Raton. DOI: 10.1201/9780203492437

Saeed, U., Dawood, U., and Ali, A. M. (2021). "Cellulose triacetate fiber-reinforced polystyrene composite," *Journal of Thermoplastic Composite Materials* 34(5), 707-721. DOI: 10.1177/0892705719847249

Sahai, R., and Pardeshi, R. (2021). "Comparative study of effect of different coupling agent on mechanical properties and water absorption on wheat straw-reinforced polystyrene composites," *Journal of Thermoplastic Composite Materials* 34(4), 433-450. DOI: 10.1177/0892705719843975

Sihombing, H., Rassiah, K., Ashaari, Z., and Yuharzi, M. Y. (2012). "Analysis and development of recycled materials for wood plastic composite product," *Elixir Mechanical Engineering* 51, 10834-10840.

Singha, A. S., and Rana, R. K. (2012). "Natural fiber reinforced polystyrene composites: Effect of fiber loading, fiber dimensions and surface modification on mechanical properties," *Materials & Design* 41, 289-297. DOI: 10.1016/j.matdes.2012.05.001

Sun, Y. Sen, Woo, E. M., Wu, M. C., and Ho, R.-M. (2003). "Polymorphism and phase transitions upon annealing in solvent-cast vs quenched syndiotactic polystyrene and its blends with atactic polystyrene," *Macromolecules* 36(22), 8415-8425. DOI: 10.1021/ma034290q

Tansel, B. (2020). "Increasing gaps between materials demand and materials recycling rates: A historical perspective for evolution of consumer products and waste quantities," *Journal of Environmental Management* 276, article 111196. DOI: 10.1016/j.jenvman.2020.111196

Ugwu, S. C., and Obele, C. M. (2023). "A mini-review on expanded polystyrene waste recycling and its applications," *World Journal of Advanced Engineering Technology and Sciences* 8(1), 315-329. DOI: 10.30574/wjaets.2023.8.1.0057

Verhaar, H. J. M., van Leeuwen, C. J., and Hermens, J. L. M. (1992). "Classifying environmental pollutants," *Chemosphere* 25(4), 471-491. DOI: 10.1016/0045-6535(92)90280-5

Wang, J., Fishwild, S. J., Begel, M., and Zhu, J. Y. (2020). "Properties of densified poplar wood through partial delignification with alkali and acid pretreatment," *Journal of Materials Science* 55(29), 14664-14676. DOI: 10.1007/s10853-020-05034-2

Wichai, K., and Vao-soongnern, V. (2021). "A multiscale simulation of amorphous polystyrene," *Journal of Polymer Research* 28(4), 109. DOI: 10.1007/s10965-021-02453-w

Yabagi, J. A., Kimpa, M. I., Muhammad, M. N., Rashid, S. Bin, Zaidi, E., and Agam, M. A. (2018). "The effect of gamma irradiation on chemical, morphology and optical

properties of polystyrene nanosphere at various exposure time," *IOP Conference Series: Materials Science and Engineering* 298, article 012004. DOI: 10.1088/1757-899X/298/1/012004

Yourtee, J. B., and Cooper, S. L. (1974). "Properties of densified amorphous polystyrene," *Journal of Applied Polymer Science* 18(3), 897-912. DOI: 10.1002/app.1974.070180323

Yuan, X., Fu, S., and Liu, H. (2025). "Preparation of wood fiber–polyurethane plastic composite with water resistance and high strength," *Materials* 18(6), article 1314. DOI: 10.3390/ma18061314

Article submitted: June 16, 2025; Peer review completed: July 26, 2025; Revised version received: July 31, 2025; Accepted: August 1, 2025; Published: August 28, 2025.
DOI: 10.15376/biores.20.4.9184-9207